Unraveling the Mechanisms of the Electronic Quenching of NO ($A^2\Sigma^+$) with CO_2 and CH_4

Aerial N. Bridgers,[1] Julia Im,[1] and Andrew S. Petit[1]

[1]Department of Chemistry and Biochemistry, California State University – Fullerton, Fullerton, CA 92834-6866, USA

Introduction

Molecular Partner	Cross Section[3]
CH_4	<0.001 Å² at 296 K
CO	6 Å² at 300 K
CO_2	68.3 Å² at 294 K
H_2O	120 Å² at 300 K

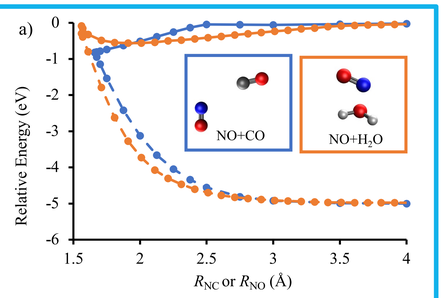

(Above) Potential energy surfaces (PESs) for both NO ($A^2\Sigma^+$)+ CO and NO ($A^2\Sigma^+$)+ H_2O. [1,2]

- Shows the relative energies of the D_1 (NO ($X^2\Pi$)+ M) and D_2 (NO ($A^2\Sigma^+$)+ M) states as a function of the intermolecular distance.
- The D_2 state of NO+ CO is less energetically attractive than NO+ H_2O.
- Stronger intermolecular interactions allow H_2O to more effectively quench NO ($A^2\Sigma^+$) than CO.
- Additionally, the D_2 PES of NO+ H_2O funnels a wide range of initial geometries into one shape, further increasing the electronic quenching.

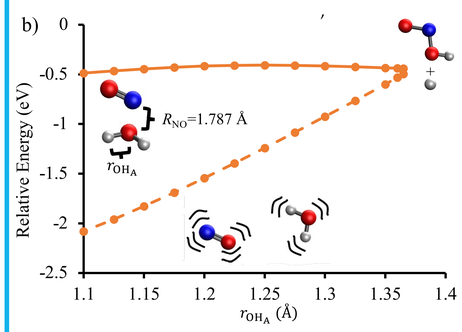

(Left) Shows the relative energies of the D_1 and D_2 states of NO+ H_2O as a function of one of the OH bond lengths of water at a fixed intermolecular distance of R_{NO}=1.787 Å. [2]

- Nonreactive quenching causes production of H_2O with a significant amount of energy in its O-H stretch
- Reactive quenching produces new species: HONO and H

Previous Work on NO ($A^2\Sigma^+$)+ CO_2 Electronic Quenching

a) Hancock and co-workers used infrared emission spectroscopy to show that 62% of the available energy partitions into the vibrational degrees of freedom of CO_2. [7]
b) 80% of the electronic quenching results in the formation of NO ($X^2\Pi$) with $v'_{NO} = 0$ or $v'_{NO} = 1$.
c) Experiments have observed reactive electronic quenching products CO and NO_2 [7]

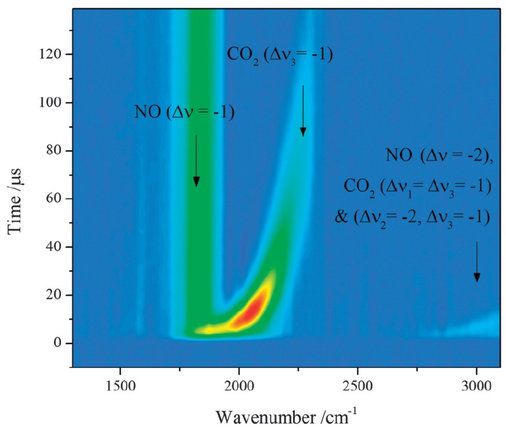

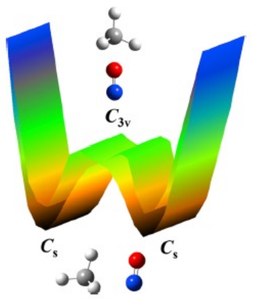

Previous Work on NO ($A^2\Sigma^+$)+ CH_4

a) NO ($X^2\Pi$)+ CH_4 is a Jahn-Teller distorted system with the NO preferentially oriented perpendicular to the intermolecular bond and undergoing large-amplitude vibrational motions. [4,5]
b) Photodissociation of NO ($X^2\Pi$)+ CH_4 produces NO ($A^2\Sigma^+$) in a broad distribution of rotational states which span the entire energetically accessible range. [6]

NO ($A^2\Sigma^+$)+ CH_4 Results

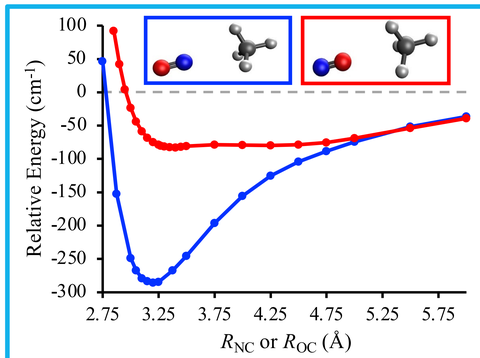

(Right) The D_0-D_5 states as function of the intermolecular distance, R_{NC}, for the ON-H_3CH complex. There is no pathway for electronic quenching at low-collision energies for NO ($A^2\Sigma^+$)+ CH_4 in the ON-H_3CH conformation.

(Left) The D_2 energies of different molecular conformations of the NO ($A^2\Sigma^+$)+ CH_4 system. The molecular geometries remained in the C_{3v} point group throughout the attractive region of the PES and only distorted to lower symmetry in the repulsive region.

- NO ($X^2\Pi$)+ CH_4 exists in a C_s conformation
- After D_0 → D_2 electronic excitation, vibrational relaxation will impart a torque on the NO as the complex reorients from C_s to C_{3v}
- This reorientation is consistent with a wide range of rotational states being present in NO ($A^2\Sigma^+$) but not in CH_4 upon photodissociation. [6]

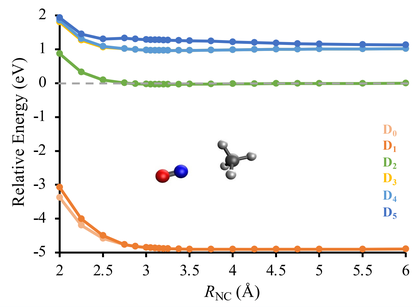

NO ($A^2\Sigma^+$)+ CO_2 Results

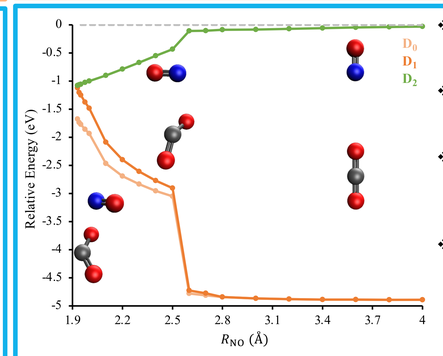

- There are multiple downhill pathways to the D_2-D_1 conical intersection
- This explains the large electronic quenching cross section for this system.
- There are significant distortions to the geometry of CO_2 observed at the approximate D_2-D_1 conical intersection.
- This is consistent with the experimental observation that NO ($A^2\Sigma^+$)+ CO_2 electronic quenching releases a large fraction of the available energy into the vibrational degrees of freedom of CO_2.

Proposed Explanation for Reactive Quenching Products:

- NO ($A^2\Sigma^+$)+ CO_2 undergoes nonreactive quenching producing vibrationally hot CO_2 and NO primarily in vibrational ground state

$$NO\ (A^2\Sigma^+) + CO_2 \rightarrow NO\ (X^2\Pi) + CO_2(\vec{v}_{CO_2} > 0)$$

- Vibrationally hot CO_2 subsequently reacts with NO and produces NO_2 and CO

$$NO\ (X^2\Pi) + CO_2(\vec{v}_{CO_2} > 0) \rightarrow NO_2 + CO$$

- If 42.96% of available energy is partitioned into CO_2 vibrational modes, then the highlighted equation becomes **exothermic**
- Experiments show that at least 62% of available energy from electronic quenching goes into CO_2 vibrational modes

NO ($A^2\Sigma^+$)+ CO_2 Results

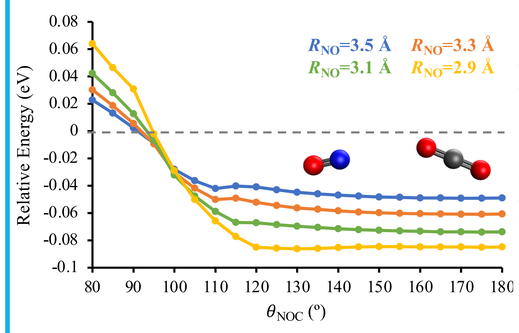

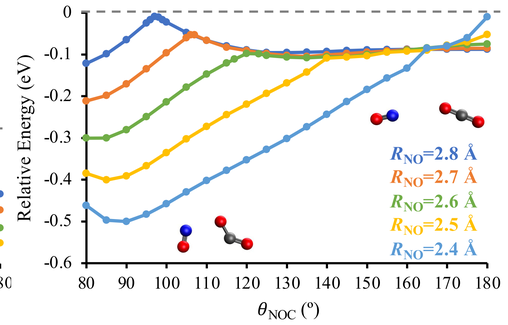

- Θ_{NOC} is the angle made by the N of NO and the C-O bond facing towards NO.
- Conformations at longer intermolecular distances are all nearly planar.
- The energy increases as Θ_{NOC} decreases, showing that the complex prefers a linear orientation at larger R_{NO}.
- Intermolecular attractions between the two molecules increase as R_{NO} decreases.
- There is a general increase in energy as Θ_{NOC} decreases until a barrier is reached.
- After the barrier, the energy sharply decreases as CO_2 adopts a bent geometry.
- As R_{NO} decreases, so does the barrier until it disappears for R_{NO}≤2.5 Å.
- The CO_2 bent conformations have strong intermolecular attractions.

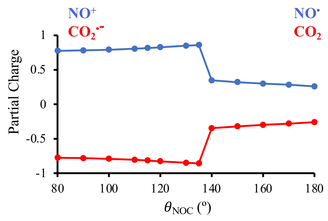

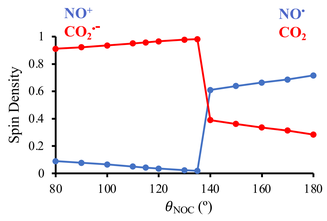

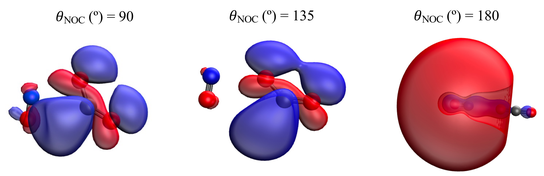

(Left) The Löwdin population analysis of the total spin densities and partial charges of NO and CO_2 as a function of Θ_{NOC} at R_{NO}=2.5 Å along with representative SOMOs for the D_2 state.

a) When CO_2 becomes bent, spin density becomes localized on CO_2 and both molecules develop significant partial charges.
b) The SOMOs further demonstrate that charge transfer occurs from NO to CO_2.
c) This is known as the harpoon mechanism.

Computational Methods

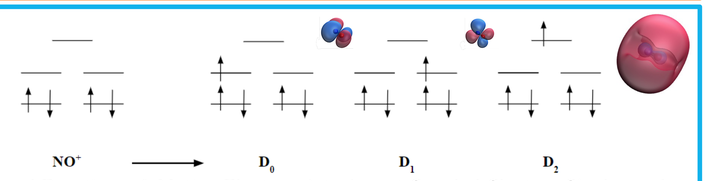

- We used Equation-of-Motion Electron Attachment Coupled Clusters Singles and Doubles (EOM-EA-CCSD) in the Q-Chem 5.0 software package.
- The EOM-EA-CCSD approach allows us to use a closed-shell reference to describe our open-shell system and describe states with valence, Rydberg, and charge-transfer character on an equal footing.[9]
- NO+ CH_4:
  - Geometry optimizations: EOM-EA-CCSD/aug-cc-pVTZ
  - Electronic energies: we used a three-point extrapolation to the complete basis set limit using AVNZ basis sets, where AVNZ is d-aug-pVNZ for N and O and aug-cc-pVNZ for C and H
- NO+ CO_2:
  - Geometry optimizations: EOM-EA-CCSD/aug-cc-pVDZ for Θ_{NOC} plots and EOM-EA-CCSD/aug-cc-pVTZ for the R_{NO} pathway to the D_2-D_1 conical intersection
  - Single-points used EOM-EA-CCSD/AVQZ, where AVQZ has d-aug-cc-pVQZ for NO and aug-cc-pVQZ for CO_2

References

1. Guardado, J.L.; Hood, D.J.; Luong, K.; Kidwell, N.M.; and Petit, A.S.; *J. Phys. Chem. A*; 2021; 125 (40); 8803-8815.
2. Guardado, J.L.; Urquilla, J.A.; Kidwell, N.M.; Petit, A.S.; *Phys. Chem. Chem. Phys.*; 2022; 24(43); 26717-26730.
3. Settersten, T.B.; Patterson, B.D.; Gray, J.A.; *J. Chem. Phys.*; 2006; 124 (23); 234308.
4. Wen, B.; Meyer, H.W.; *J. Chem. Phys.*; 2009; 131 (3); 034304.
5. Davis, J.P.; Neisser, R.W.; Kidwell, N.M.; *J. Phys. Chem. A*; 2023;127 (24); 5171-5182.
6. Holmes-Ross, HL; Gascooke, J.R.; Lawrance, W.D.; *J. Phys Chem A*; 2022; 126 (43); 7981-7996.
7. Burgos, P.; Few, J.; Gowrie, S.; Hancock, G.; *Phys. Chem. Chem. Phys.*; 2013; 15 (7); 2554.
8. Bridgers, A.N.; Urquilla, J.A.; Im, J.; Petit, A.S.; *J. Phys. Chem. A*; 2023; In Press.
9. Krylov, A. I. Annu. Rev. *Phys. Chem.* 2008, 59 (1), 433-462.

Acknowledgements

- Special thanks to Dr. Petit and members of the Petit group.
- Thanks to the Center for Computational and Applied Mathematics (CCAM).
- Thanks to CSUF's Chemistry and Biochemistry Department.